This article is a *Plant Cell* Advance Online Publication. The date of its first appearance online is the official date of publication. The article has been edited and the authors have corrected proofs, but minor changes could be made before the final version is published. Posting this version online reduces the time to publication by several weeks.

Cyanobacterial Lactate Oxidases Serve as Essential Partners in N_2 Fixation and Evolved into Photorespiratory Glycolate Oxidases in Plants [W]

Claudia Hackenberg,[a] Ramona Kern,[a] Jan Hüge,[b] Lucas J. Stal,[c] Yoshinori Tsuji,[d] Joachim Kopka,[b] Yoshihiro Shiraiwa,[d] Hermann Bauwe,[a] and Martin Hagemann[a,1]

[a] University of Rostock, Plant Physiology Department, 18051 Rostock, Germany
[b] Max-Planck-Institute of Molecular Plant Physiology, 14476 Potsdam-Golm, Germany
[c] Department of Marine Microbiology, Netherlands Institute of Ecology (NIOO-KNAW), Centre for Estuarine and Marine Ecology, 4400 AC Yerseke, The Netherlands
[d] Laboratory of Plant Physiology and Metabolism, Graduate School of Life and Environmental Sciences, University of Tsukuba, Tsukuba 305-8572, Japan

Glycolate oxidase (GOX) is an essential enzyme involved in photorespiratory metabolism in plants. In cyanobacteria and green algae, the corresponding reaction is catalyzed by glycolate dehydrogenases (GlcD). The genomes of N_2-fixing cyanobacteria, such as *Nostoc* PCC 7120 and green algae, appear to harbor genes for both GlcD and GOX proteins. The GOX-like proteins from *Nostoc* (No-LOX) and from *Chlamydomonas reinhardtii* showed high L-lactate oxidase (LOX) and low GOX activities, whereas glycolate was the preferred substrate of the phylogenetically related At-GOX2 from *Arabidopsis thaliana*. Changing the active site of No-LOX to that of At-GOX2 by site-specific mutagenesis reversed the LOX/GOX activity ratio of No-LOX. Despite its low GOX activity, No-LOX overexpression decreased the accumulation of toxic glycolate in a cyanobacterial photorespiratory mutant and restored its ability to grow in air. A LOX-deficient *Nostoc* mutant grew normally in nitrate-containing medium but died under N_2-fixing conditions. Cultivation under low oxygen rescued this lethal phenotype, indicating that N_2 fixation was more sensitive to O_2 in the Δ*lox Nostoc* mutant than in the wild type. We propose that LOX primarily serves as an O_2-scavenging enzyme to protect nitrogenase in extant N_2-fixing cyanobacteria, whereas in plants it has evolved into GOX, responsible for glycolate oxidation during photorespiration.

INTRODUCTION

Cyanobacteria evolved approximately three billion years ago and were the first organisms that performed oxygenic photosynthesis. This important metabolic process was later transferred into a eukaryotic host through an endosymbiotic event, eventually leading to the evolution of algae and land plants (Mereschkowsky, 1905; Margulis, 1970; Reyes-Prieto et al., 2007). Hence, many plant genes originated from the cyanobacterial endosymbiont, including those coding for proteins involved in photosynthesis and many other metabolic and regulatory functions (Martin et al., 2002). Phylogenetic studies have indicated that the primary endosymbiont was closely related to extant filamentous, heterocystous, N_2-fixing cyanobacteria (Deusch et al., 2008), such as *Nostoc* (*Anabaena*) sp strain PCC 7120 (hereafter *Nostoc*).

All organisms performing oxygenic photosynthesis use the Calvin-Benson cycle for CO_2 fixation with ribulose-1,5-bis-phosphate carboxylase/oxygenase as the carboxylating enzyme, producing two molecules of 3-phosphoglycerate. In addition to its carboxylase activity, ribulose-1,5-bis-phosphate carboxylase/oxygenase acts as an oxygenase and produces 2-phosphoglycolate (2PG) in the presence of O_2. 2PG is toxic and becomes converted to 3-phosphoglycerate by a process known as photorespiration (Husic et al., 1987; Bauwe et al., 2010). Mutations in the enzymatic steps of the photorespiratory cycle in most cases result in lethal phenotypes at ambient CO_2 levels but can be rescued under high CO_2 levels, when the oxygenase reaction is suppressed (Blackwell et al., 1988; Somerville, 2001). This high-CO_2-requiring (HCR) phenotype is characteristic of mutants defective in 2PG metabolism and is known as the photorespiratory phenotype. Accordingly, in the current atmosphere, plants can perform oxygenic photosynthesis only in the presence of a fully operational photorespiratory cycle. This is true for both C_3 plants and C_4 plants. Mutants of the C_4 plant maize (*Zea mays*) with deletion of the photorespiratory enzyme glycolate oxidase (GOX) also exhibit an HCR phenotype (Zelitch et al., 2009).

Because cyanobacteria possess an efficient inorganic carbon concentrating mechanism (CCM), it was assumed that they do not perform photorespiratory 2PG metabolism (reviewed in Colman, 1989; Giordano et al., 2005). Cyanobacterial CCM mutants exhibit an HCR phenotype (reviewed in Kaplan and Reinhold, 1999; Badger et al., 2006). More recent studies have

[1] Address correspondence to martin.hagemann@uni-rostock.de.
The author responsible for distribution of materials integral to the findings presented in this article in accordance with the policy described in the Instructions for Authors (www.plantcell.org) is: Martin Hagemann (martin.hagemann@uni-rostock.de).
[W] Online version contains Web-only data.
www.plantcell.org/cgi/doi/10.1105/tpc.111.088070

revealed that active photorespiratory 2PG metabolism is present in the cyanobacterium *Synechocystis* sp strain PCC 6803 (hereafter *Synechocystis*). This organism employs three routes for 2PG detoxification: (1) a plant-like 2PG cycle, (2) the glycerate pathway, and (3) the decarboxylation of glyoxylate via formate. The combined loss of all three routes resulted in an HCR phenotype and demonstrated the essential function of photorespiratory 2PG metabolism in *Synechocystis*, despite the presence of a CCM. These findings led to the hypothesis that primary endosymbiosis conveyed not only oxygenic photosynthesis but also an ancient photorespiratory 2PG metabolism into the eukaryotic host (Eisenhut et al., 2008a).

Several differences between the photorespiratory 2PG metabolism of *Synechocystis* and land plants have been noted (reviewed in Bauwe et al., 2010). For example, the oxidation of glycolate to glyoxylate in *Synechocystis* (and many other cyanobacteria) is mediated by two glycolate dehydrogenases (GlcDs) that use $NAD(P)^+$ as cofactor. Similarly, in green algae, this reaction is also performed by GlcD (Codd et al., 1969; Nelson and Tolbert, 1970; Frederick et al., 1973). Correspondingly, the knockout of GlcDs in *Synechocystis* (Eisenhut et al., 2008a) or in the green alga *Chlamydomonas reinhardtii* (Nakamura et al., 2005) results in an HCR phenotype. In land plants, peroxisome-localized GOX catalyzes the glycolate oxidation, using molecular oxygen as a cosubstrate. Five isoforms of GOX proteins are imported into the peroxisome of *Arabidopsis thaliana*. Among them, isoform 2, GOX2 (At3g14415), is thought to play a major role in the photorespiratory glycolate oxidation step (Reumann et al., 2004; Bauwe et al., 2010). The diversity of photorespiratory strategies among oxygenic phototrophic organisms could reflect a stepwise loss, modification, and/or acquisition of enzymes.

In a recent phylogenetic study of enzymes possibly involved in the plant-like 2PG metabolism (Kern et al., 2011), we found that the genomes of N_2-fixing cyanobacteria and green algae contain genes similar to both types of glycolate-oxidizing enzymes, GlcD and plant-like GOX. We hypothesized that the plant GOX family could possibly originate from an ancestral cyanobacterial protein. Here, we report on a functional characterization of the corresponding GOX-like proteins from the N_2-fixing *Nostoc* strain (No-LOX, gene *all*0170 or *lox*) and *C. reinhardtii* (Cr-LOX). Additionally, we analyzed the importance of the No-LOX for the diazotrophic growth of *Nostoc*. Our results suggest that an ancestral cyanobacterial LOX may have evolved to perform two different functions. In extant N_2-fixing cyanobacteria such as *Nostoc*, it serves as an O_2-scavenging enzyme, protecting nitrogenase. After endosymbiotic transfer, the enzyme was successively modified in the plant lineage to use glycolate as its preferred substrate in the photorespiratory cycle.

RESULTS

Phylogenetic Analysis of GOX

To analyze the evolutionary history of GOX enzymes in silico, we extended an earlier study (Kern et al., 2011) using *Arabidopsis* GOX2 (At3G14415) as a target sequence in BLASTP searches to identify a broad range of related proteins in bacteria, including cyanobacteria, algae, and plants. These putative GOX enzymes included the *Nostoc* protein encoded by gene *all*0170, which was used as a target sequence in a second set of BLASTP searches. An unrooted phylogenetic tree (Figure 1), constructed from the

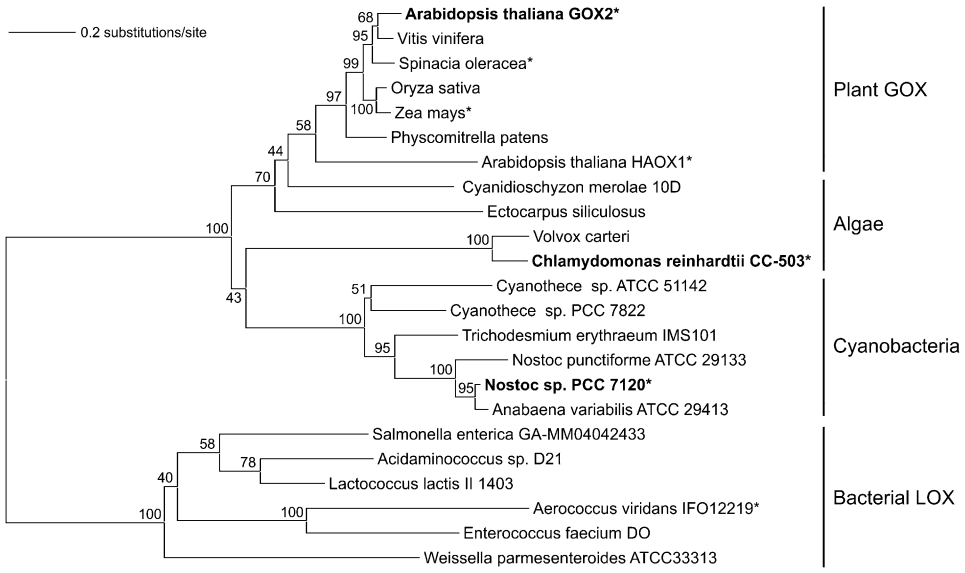

Figure 1. Phylogenetic Relationship between GOX and LOX Proteins.

Neighbor-joining tree of putative GOX or LOX proteins [(*S*)-2-hydroxy-acid oxidase, EC 1.1.3.15] based on 23 sequences. Numbers at the node indicate bootstrap values (percentage) for 1000 replicates. The distance scale (substitutions per site) is shown in the top left-hand corner. Asterisks refer to biochemically characterized enzymes (Macheroux et al., 1992; Maeda-Yorita et al., 1995; Eprintsev et al., 2009). Proteins shown in boldface were analyzed in this study. The alignment used for this analysis is available as Supplemental Data Set 1 online.

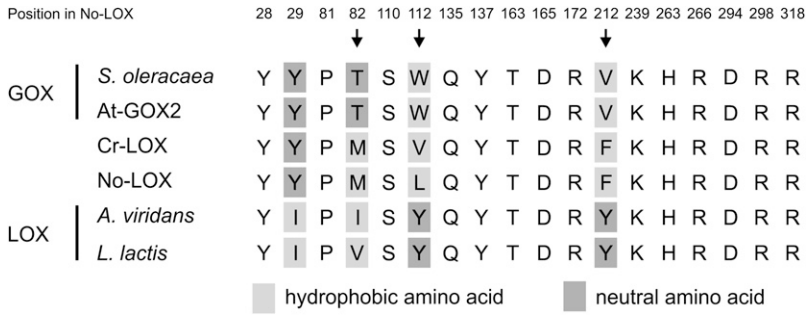

Figure 2. Comparative Analysis of Amino Acid Exchanges in the Active Sites of GOXs and LOXs.

The given amino acid positions refer to the enzyme from *Nostoc* (No-LOX, All0170; the full alignment is shown Supplemental Figure 1 online). The residues involved in the binding of FMN are highly conserved between both enzyme types (Lindqvist and Brändén, 1989; Maeda-Yorita et al., 1995; Stenberg et al., 1995; Stenberg and Lindqvist, 1997; Leiros et al., 2006). Amino acids presumably involved in substrate binding are marked in gray. Arrows mark amino acid changes in No-LOX variants by site-specific mutagenesis.

identified sequences, all belonging to a protein family of (*S*)-2-hydroxy-acid oxidases (EC 1.1.3.15), displayed two main clusters. One cluster includes the structurally and biochemically characterized GOX from spinach (*Spinacia oleracea*; Lindqvist, 1989) and many other plants together with uncharacterized cyanobacterial and algal proteins, which may be considered as GOX-like sequences. The second cluster included many bacterial proteins known to exhibit LOX activity, for example, *Aerococcus viridans* LOX (Maeda-Yorita et al., 1995). Their close relationship is also reflected by the similar structures of their active sites. Selected bacterial, cyanobacterial, algal, and plant proteins from the two clusters possess only a few alterations with respect to the amino acid residues in their active sites (Figure 2).

The existence of a clade containing only cyanobacterial proteins and proteins from photosynthetic eukaryotes (green plants, green algae, red algae, and brown algae), which is statistically supported by bootstrap values of 100% (Figure 1), is indicative of a cyanobacterial origin of all these proteins in eukaryotic phototrophs. Correspondingly, the cyanobacterial protein from *Nostoc* (All0170) has a higher overall similarity to the *Arabidopsis* GOX2 and the spinach GOX (70 and 62% sequence identity, respectively) compared with the LOX enzymes from the heterotrophic bacteria *Lactococcus lactis* and *A. viridans* (57 and 55% sequence identity, respectively) (see Supplemental Figure 1 online).

Interestingly, genes encoding cyanobacterial GOX-like proteins were exclusively found in the genomes of N_2-fixing species; they were absent from the genomes of nondiazotrophic cyanobacteria. It should be noted that, in addition to these putative GOX-encoding sequences, all genomes of N_2-fixing cyanobacteria also harbor one or two genes coding for glycolate dehydrogenases that are highly similar to the photorespiratory GlcD1 and GlcD2 proteins from *Synechocystis* (Eisenhut et al., 2008a). The coexistence of genes coding for GlcDs (e.g., *alr*5269 - *glcD1* and *all*4443 - *glcD2* in *Nostoc*) and GOX-like proteins (e.g., *all*0170 in *Nostoc*) in all sequenced genomes of N_2-fixing cyanobacteria was unexpected and raised two questions. Are cyanobacterial GOX-like proteins capable of oxidizing glycolate to glyoxylate? What are the cellular functions of these proteins?

Biochemical Analyses of GOX-Like Proteins in Vitro

To verify the enzymatic activity of the cyanobacterial GOX-like proteins in comparison to a plant GOX, the proteins from *Nostoc* and GOX2 from *Arabidopsis* were overexpressed in *Escherichia coli* using the corresponding gene (*Nostoc*) or cDNA (*Arabidopsis*) in combination with the overexpression vector pET-28a. Virtually pure His-tagged proteins were obtained (see Supplemental Figure 2 online) and examined for catalytic activities with a range of potential substrates, each at 5 mM concentration (Table 1). Both enzymes catalyzed oxidase reactions, consuming O_2 and producing H_2O_2 as byproduct, but neither showed any dehydrogenase activity with NAD^+ or $NADP^+$. In this experiment, the cyanobacterial enzyme showed an ~200-fold higher activity with L-lactate in comparison to glycolate, whereas the plant At-GOX2 was ~10-fold more active with glycolate than L-lactate. The clear preference for L-lactate over glycolate showed that the cyanobacterial enzyme is a LOX rather than a GOX; therefore, it was named No-LOX. Neither of the two enzymes accepted D-lactate as a substrate (Table 1), which has been reported previously for plant and algal GOX (Frederick et al., 1973).

Table 1. Enzyme Activities of Recombinant No-LOX and At-GOX2 with Different Substrates

	Relative Specific Activity (%)	
Substrate (5 mM)	No-LOX	At-GOX2
Glycolate	0.44 ± 0.06	100
L-lactate	100	12.58 ± 5.29
D-lactate	0	0
Glyoxylate	15.33 ± 3.92	0
Glycerate	5.89 ± 2.77	9.96 ± 5.61
Hydroxypyruvate	0.33 ± 0.11	18.81 ± 4.22

Enzyme activities were measured under the standard assay conditions described in Methods. One hundred percent activity is defined for 5 mM of the substrates L-lactate (No-LOX: 14.73 ± 3.59 μmol min^{-1} mg^{-1}) or glycolate (At-GOX2: 24.27 ± 5.00 μmol min^{-1} mg^{-1}). Parameters represent the mean ± SD of at least three independent enzyme preparations.

Table 2. Kinetic Parameters of Recombinant No-LOX, Cr-LOX, and At-GOX2

	L-Lactate		Glycolate	
Enzyme	K_m (mM)	V_{max} (μmol min^{-1} mg^{-1})	K_m (mM)	V_{max} (μmol min^{-1} mg^{-1})
No-LOX	0.039 ± 0.007	12.73 ± 1.55	0.233 ± 0.05	0.049 ± 0.021
Cr-LOX	0.081 ± 0.027*	10.59 ± 0.46	1.244 ± 0.063*	0.189 ± 0.059*
At-GOX2	0.356 ± 0.182*	0.742 ± 0.036*	1.906 ± 0.64*	35.64 ± 11.16*

Kinetic parameters were calculated by nonlinear regression fit to the Michaelis-Menten equation (Sigma Plot software) or by linear regression analysis of the double-reciprocal data pairs (Lineweaver-Burk). Parameters represent the mean ± SD of at least three independent enzyme preparations. Statistically significant differences from No-LOX (asterisk) are indicated ($P < 0.1$ or better).

No-LOX, but not At-GOX2, showed clear oxidase activity with glyoxylate. To a minor degree, both enzymes also accepted glycerate and hydroxypyruvate as substrates (Table 1).

Next, we examined the kinetic parameters of these two enzymes in addition to those of the homologous protein from the green alga *C. reinhardtii*. GOX-like proteins from green algae could shed light on where in the phylogenetic tree enzyme activity evolution occurred (Figure 1). Sequence analyses of several independent cDNA clones, obtained from total RNA of *C. reinhardtii* grown under photoautotrophic, low-carbon conditions, revealed that the nucleotide sequence differs from that in the database (XP_001703481) by six additional nucleotides. This is probably due to the misannotation of a splice site in the corresponding gene (accession number of the corrected cDNA sequence at DDBJ: AB610509). As found before with the cyanobacterial enzyme No-LOX, the enzyme from *Chlamydomonas* has higher affinities for L-lactate than for glycolate as substrate (Table 2) and was named Cr-LOX. With respect to the calculated substrate-saturated rates, the estimated kinetic parameters of the enzymes confirmed the results obtained from the experiment with fixed substrate concentrations (Table 1). The V_{max} of L-lactate oxidation by No-LOX was >200-fold higher than that of glycolate oxidation (Table 2). By contrast, At-GOX2 exhibited a 40 times higher V_{max} for glycolate than for L-lactate. The affinity of No-LOX for L-lactate but also for glycolate is significantly higher than that of At-GOX2 (Table 2). With respect to all four kinetic parameters, the enzyme from *Chlamydomonas* is positioned between No-LOX and At-GOX2, but with the exception of the K_m for glycolate it is more similar to the cyanobacterial enzyme.

Additionally, the affinity of No-LOX for the cosubstrate O_2 was estimated. No-LOX activity was followed under decreasing oxygen concentrations at saturating L-lactate concentrations. These experiments revealed a very high affinity for O_2 (K_m value of 0.29 ± 0.14 μM O_2; $n = 21$) of the recombinant No-LOX protein.

To identify the amino acid exchanges that were most important to L-lactate versus glycolate preference, we compared the likely substrate binding site of No-LOX with those of the bacterial LOX and plant GOX enzymes and found alterations in four positions, three of which corresponded to amino acids involved in flavin mononucleotide (FMN) and/or substrate binding (positions 82, 112, and 212 in Figure 2). Next, we replaced these three amino acids in the No-LOX sequence, both individually and in combinations of two or all three, with the corresponding amino acids in the plant GOX consensus sequence. The resulting seven mutated No-LOX variants were overexpressed in *E. coli*, purified, and examined for changes in their reactivities with glycolate and L-lactate (Table 3). With the exception of the variant M82T, which showed higher activities with both substrates in comparison to wild-type No-LOX, the oxidation of L-lactate was considerably impaired in all variants. By contrast, glycolate reactivities improved in most variants, including the triple mutant. The double mutants M82T/L112W and L112W/F212V showed up to 10-fold increased GOX activities. Moreover, the LOX/GOX activity ratios of all variants decreased considerably and came very close to that of At-GOX2 in the double mutant L112W/F212V and the triple mutant (Table 3).

Complementation of the Double Mutant Δ*glcD1/D2* of *Synechocystis* by No-LOX

Previously, we have shown that deletion of GlcD in *Synechocystis*, a cyanobacterium not capable of N_2 fixation and missing a

Table 3. Enzyme Activities of Wild-Type Enzymes and Amino Acid Substitution Variants of No-LOX with Glycolate and L-Lactate as Substrates

	Activity (μmol min^{-1} mg^{-1})		Ratio
Enzyme Variant	Glycolate (5 mM)	L-Lactate (5 mM)	L-Lactate/ Glycolate
Wild-type enzymes			
No-LOX	0.06 ± 0.01	14.73 ± 3.59	245.5
Cr-LOX	0.16 ± 0.06	9.75 ± 0.46	60.9
At-GOX2	24.27 ± 5.00	3.05 ± 1.28	0.1
Single substitution in No-LOX			
M82T	0.55 ± 0.10	23.34 ± 2.76	42.5
L112W	0.06 ± 0.02	7.69 ± 0.48	120.2
F212V	0.16 ± 0.03	1.43 ± 0.30	9.0
Double substitution in No-LOX			
M82T, L112W	0.11 ± 0.06	0.47 ± 0.04	4.2
M82T, F212V	0.47 ± 0.13	7.57 ± 1.10	16.3
L112W, F212V	0.60 ± 0.13	0.38 ± 0.07	0.6
Triple substitution in No-LOX			
M82T, L112W, F212V	0.26 ± 0.04	0.11 ± 0.03	0.4

Enzyme activities were measured using the standard assay conditions described in Methods. The activities of the unchanged recombinant enzymes from *Nostoc*, *Arabidopsis*, and *Chlamydomonas* (wild-type enzymes, Table 1) are shown for comparison. Parameters represent the mean ± SD of at least three independent enzyme preparations.

GOX-like protein, resulted in an HCR phenotype (Eisenhut et al., 2008a). The *Synechocystis* double mutant Δ*glcD1/D2* was chosen as a host for complementation with No-LOX, in comparison with At-GOX2 as a control, to evaluate the potential involvement of No-LOX in photorespiratory glycolate oxidation in vivo. The genotypes of strains expressing the genes *all*0170 (No-LOX) or the cDNA for *At3g14415* (At-GOX2) were characterized by PCR (Figure 3A). These analyses verified the complete segregation of the *glcD1* and *glcD2* mutations, as observed in the parental strain Δ*glcD1/D2*, and the presence of the No-LOX expression vector (in the complemented strain Δ*glcD1/D2*+No-LOX) or the At-GOX2 expression vector (in the complemented strain Δ*glcD1/D2*+At-GOX2). We also confirmed that neither of the overexpression vectors was present in the parental double mutant. Expression levels were examined by immunoblotting using specific antibodies raised against No-LOX and At-GOX2 (Figure 3B). Cross-reacting signals were obtained only in the complemented strains, not in the wild type or the cells of the noncomplemented parental double mutant. The observed expression levels of No-LOX or At-GOX2, respectively, were unaffected by cultivation at low or high CO_2 conditions (LC or HC).

Previous results showed that stepwise increases in glycolate accumulation in the single and double *glcD*-mutants of *Synechocystis* (Δ*glcD2* < Δ*glcD1* < Δ*glcD1/D2*) were accompanied by stepwise decreases in growth rates, ranging from the slightly impaired growth of the single mutants to the HCR phenotype of the Δ*glcD1/D2* double mutant (Eisenhut et al., 2008a). The expression of At-GOX2 or No-LOX complemented this HCR phenotype (Figure 4). The No-LOX–expressing double mutant was able to grow ($\mu = 0.006 \pm 0.002\ h^{-1}$) in a similar manner to the Δ*glcD1* single-mutant ($\mu = 0.005 \pm 0.002\ h^{-1}$), suggesting that the glycolate-to-glyoxylate conversion rate of No-LOX is similar to that of *Synechocystis* GlcD2 in vivo. Indeed, the internal glycolate concentration in the No-LOX–expressing strain decreased by ~60%, compared with the Δ*glcD1/D2* double mutant (Figure 4C), which was similar to the glycolate levels reported for the single mutant Δ*glcD1* (Eisenhut et al., 2008a). In correlation with the much higher activity of At-GOX2 observed with glycolate, the strain expressing this plant enzyme showed significantly higher growth rates, reaching those of wild-type cells ($\mu = 0.011 \pm 0.002\ h^{-1}$). Notably, this strain accumulated only traces of glycolate, similar to the *Synechocystis* wild type (Figure 4).

Generation and Characterization of a *Nostoc* Δ*lox* Mutant

To analyze the function of No-LOX in its natural host, *Nostoc*, a targeted mutation of *all*0170 (*lox*) was performed. We obtained several independent spectinomycin (Sp)-resistant and Suc-resistant clones. A genotypic characterization of these lines by PCR (see Supplemental Figure 3 online) revealed that the wild-type copy was completely absent in the *Nostoc* Δ*lox* mutant (Δ*all*0170::Sp). Only disrupted mutant gene copies were detected. The phylogenetically related GOX proteins play an important

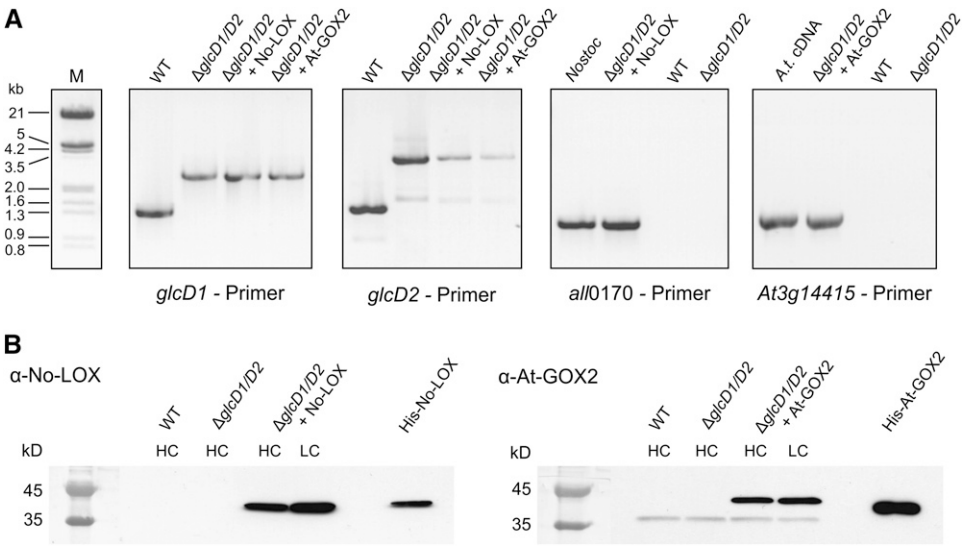

Figure 3. Genotypic Characterization of Strains Used in the Complementation Experiment of the *Synechocystis* Δ*glcD1/D2* Double Mutant with No-LOX or At-GOX2.

(A) Genotypic characterization of Δ*glcD1/D2*+No-LOX and Δ*glcD1/D2*+At-GOX2. Complete segregation of the genes *glcD1* and *glcD2* in the parental *Synechocystis* strain Δ*glcD1/D2* and the complemented strains, respectively, and detection of *all*0170 (encoding No-LOX) and *At3g14415* (encoding At-GOX2) in the complemented strains was verified with gene-specific primers (see Supplemental Table 2 online). M, size marker (λ-DNA *Eco*RI/*Hin*dIII); WT, wild type.

(B) Immunoblotting analysis with protein extracts from cells of *Synechocystis* wild type, Δ*glcD1/D2*, Δ*glcD1/D2*+No-LOX, and Δ*glcD1/D2*+At-GOX2 to confirm the expression of No-LOX and At-GOX2 in the respective complemented strains with the corresponding antibodies. Cells were cultivated at either CO_2-enriched (HC) or ambient air (LC) conditions. Ten micrograms of total soluble protein fraction was applied per lane. The heterologously expressed enzymes served as positive controls (His-No-LOX and His-At-GOX2).

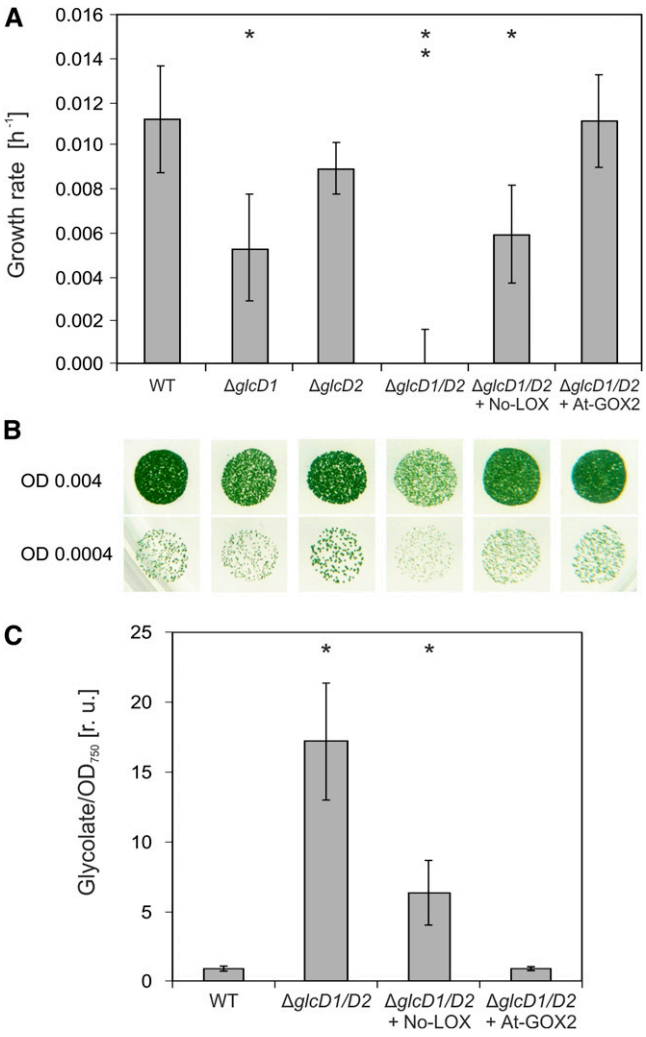

Figure 4. Phenotypic Characterization of *Synechocystis* Δ*glcD1/D2* Mutants Overexpressing No-LOX or At-GOX2.

(A) and **(B)** Growth of the *Synechocystis* wild type (WT), single, and double *glcD* mutants and the GOX-complemented strains Δ*glcD1/D2*-No-LOX and Δ*glcD1/D2*-At-GOX2, respectively, was analyzed in liquid media **(A)** and on agar plates **(B)** under ambient air (LC) conditions.

(C) Quantification of intracellular glycolate in cells of *Synechocystis* wild type, double mutant Δ*glcD1/D2*, and the two complemented strains after 24 h at LC conditions. r.u., relative units.

Bar graphs represent mean and SD of three independent biological replicates for each experiment. Statistically significant differences in the growth rate compared with the wild type (asterisk) and corresponding single mutant (double asterisk) cells are indicated ($P < 0.05$).

role during the photorespiration of land plants, and its deletion results in an HCR phenotype (Zelitch et al., 2009). Therefore, we first examined whether the *Nostoc* mutant Δ*lox* expresses an HCR phenotype similar to that of the GlcD-deficient mutants of *Synechocystis*. After cultivation in nitrate-containing BG11 medium under both LC and HC conditions, however, the Δ*lox*-mutant exhibited growth rates similar to wild-type *Nostoc*.

Due to the restriction of GOX-like proteins to extant cyanobacteria capable of fixing atmospheric N_2 (Figure 1), we reasoned that these enzymes may be most important under diazotrophic growth conditions. For example, No-LOX could play a role in the metabolism of the *Nostoc* heterocysts. These are specialized cells that harbor nitrogenase and are responsible for the fixation of N_2 (reviewed in Kumar et al., 2010). Since nitrogenase is extremely sensitive to O_2, heterocysts provide the anoxic environment required for this enzyme to function. As an O_2-consuming enzyme, No-LOX could possibly contribute to a decrease in O_2 partial pressure inside heterocysts. To test this hypothesis, we transferred cells from the *Nostoc* wild type and mutant Δ*lox* to diazotrophic growth conditions in liquid and on solid media (Figure 5). During the first 48 h following the shift to nitrate-free conditions, the mutant showed similar growth rates compared with the wild type (Figure 5A). After 72 h, while wild-type cells continued to grow, the growth rate of the Δ*lox* mutant decreased, and the cells bleached completely after 120 h. The same phenomenon was observed when the mutant Δ*lox* was grown on agar plates: Δ*lox* formed yellowish colonies in the first week but completely bleached out after 2 weeks in the absence of a combined nitrogen source, while wild-type colonies were capable of growing (Figure 5B). These results show that the *Nostoc* Δ*lox* mutant was unable to grow diazotrophically.

To assess the failure of the *Nostoc* Δ*lox* mutant in fixing N_2, we quantified the heterocyst formation. Light microscopy analyses 48 h after the shift to nitrate-free conditions revealed that filaments of the mutant Δ*lox* contained morphologically normal heterocysts in the same frequency as the wild-type *Nostoc* (9.45% ± 0.49% heterocysts in filaments of Δ*lox*, 9.3% ± 0.24% heterocysts in wild-type filaments).

Next, we shifted wild-type *Nostoc* and Δ*lox* cells to nitrate-free, microaerobic conditions (maintained by flushing bicarbonate-supplemented cultures continuously with N_2) to verify that the inability of Δ*lox* to grow diazotrophically was caused by the inability of this mutant to protect nitrogenase from O_2 inhibition. Under these conditions, the mutant did not bleach and grew at levels similar to the wild type, indicating that they had switched to diazotrophic growth (Figure 5C) and indicating a possible role of No-LOX in the protection of nitrogenase by the scavenging of O_2 in heterocysts.

To obtain additional evidence to test this hypothesis, we performed acetylene reduction assays to measure nitrogenase activity in vivo. After 24 and 72 h in nitrate-free medium, $BG11_0$, aliquots of cells were taken and incubated at different oxygen concentrations during nitrogenase activity measurements. Despite the relatively high deviations of the nitrogenase activities, the two data sets showed similar changes in the oxygen sensitivity of nitrogenase in intact filaments. *Nostoc* wild-type cells exhibited maximum nitrogenase activities at ambient conditions of 20% O_2 (up to 160 μmol C_2H_4 g^{-1} chlorophyll *a* h^{-1}), and lower rates were observed at both lower and higher O_2 concentrations (Table 4). By contrast, the nitrogenase activity of the Δ*lox* mutant was highest in the absence of O_2. With increased O_2 concentrations, the nitrogenase activity of Δ*lox* decreased. In 20% O_2 of ambient air, the nitrogenase activity of the mutant Δ*lox* was significantly lower than in the *Nostoc* wild-type cultures.

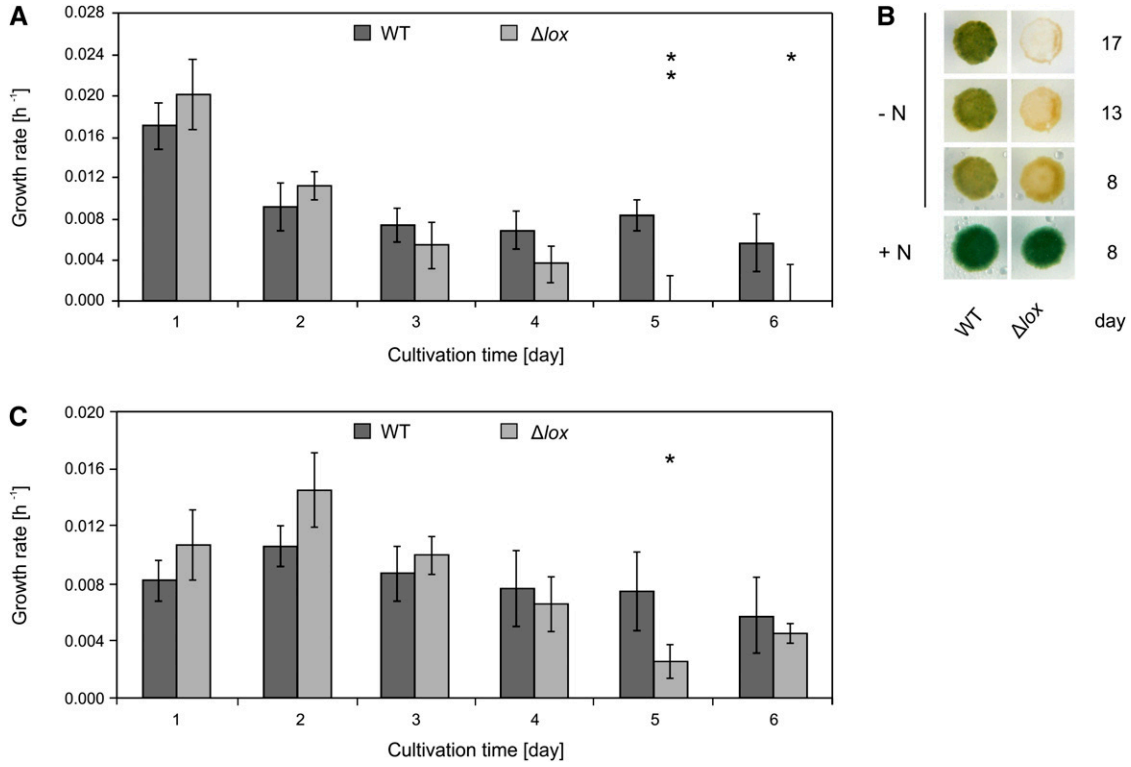

Figure 5. Phenotypic Characterization of *Nostoc* Wild Type and Mutant Δ*lox* Grown at Different Conditions.

(A) and **(B)** Cells were transferred from nitrate-containing medium BG11 (+N) into nitrate-free medium $BG11_0$ (-N) at time point 0 in liquid cultures under CO_2-enriched (HC) conditions **(A)** or onto agar plates at ambient air (LC) conditions **(B)**. WT, wild type.

(C) Alternatively, cells in liquid cultures were transferred from nitrate-containing medium BG11 into nitrate-free medium $BG11_0$ supplemented with 10 mM HCO_3^- at time point 0 at microaerobic conditions obtained by bubbling with pure N_2.

Bar graphs represent mean and SD of five independent biological replicates for each experiment. Statistically significant differences between the wild type and Δ*lox* are indicated (*$P < 0.05$ and **$P < 0.01$).

DISCUSSION

GOX catalyzes the oxygen-dependent oxidation of glycolate to glyoxylate and is known to be an essential peroxisomal enzyme in photorespiratory metabolism in land plants (for example, Clagett et al., 1949; Zelitch et al., 2009). Until recently, glycolate oxidation in cyanobacteria and green algae was more or less exclusively attributed to glycolate dehydrogenases (EC 1.1.99.14) (Codd et al., 1969; Nelson and Tolbert, 1970; Frederick et al., 1973; Beezley et al., 1976; Eisenhut et al., 2008a; Atteia et al., 2009). These glycolate dehydrogenases are similar to the GlcD subunit of *E. coli* glycolate dehydrogenase, also sometimes referred to as GOX (Pellicer et al., 1996), which allows for this heterotrophic bacterium to use glycolate as a carbon source via the glycerate pathway. In most cyanobacteria, this pathway provides one of three routes for the recovery of photorespiratory glycolate (Eisenhut et al., 2008a; Bauwe et al., 2010). By contrast, glycolate oxidation via GOX was thought to be specific to land plants and not present in other oxygenic phototrophs, with the possible exception of some streptophyte algae (Stabenau and Winkler, 2005; Chauvin et al., 2008). Therefore, the presence of glycolate dehydrogenases was considered to be an ancestral feature that was replaced by GOX in the land plant lineage. Our phylogenetic and subsequent biochemical analyses provide evidence that functional 2-hydroxy-acid oxidases with low GOX activity are also present in green algae and in N_2-fixing cyanobacteria but that the *Nostoc* and *Chlamydomonas* enzymes No-LOX and Cr-LOX, respectively, use L-lactate rather than glycolate as their preferred substrate. A close relationship between GOX and LOX was not surprising because both enzymes use FMN as cofactors and short-chain hydroxyl acids as substrates (Lindqvist and Brändén, 1989; Maeda-Yorita et al., 1995; Leiros et al., 2006). Moreover, the phylogenetic relation of cyanobacterial, algal, and plant GOX-like proteins implies that the ancestor of the plant GOX family was acquired from the primary endosymbiotic event. Therefore, the GOX family represents another example of the endosymbiotic transfer of proteins for oxygenic photosynthesis and for the ability to detoxify photorespiratory glycolate, two closely related metabolic processes.

Our studies show that glycolate became the preferred substrate at some point in the evolution of plants. The V_{max} of No-LOX for glycolate was ~700-fold lower when compared with the plant GOX (Table 2). However, the affinity of No-LOX for glycolate is similar to the reported values for GOX from pea (*Pisum*

Table 4. Nitrogenase Activity of Cells of the *Nostoc* Wild Type and Mutant Δ*lox*

	Nitrogenase Activity (μmol C_2H_4 g^{-1} Chla h^{-1})			
	24 h $BG11_0$		72 h $BG11_0$	
Oxygen (%)	Wild Type	Δ*lox*	Wild Type	Δ*lox*
0	23.2 ± 1.2	85.1 ± 9.9*	55.9 ± 10.6	76.1 ± 42.7
5	24.1 ± 5.5	35.0 ± 2.0	52.9 ± 44.7	68.8 ± 18.6
10	34.2 ± 23.9	41.5 ± 1.2	51.2 ± 3.0	29.9 ± 10.5
15	20.4 ± 9.5	19.1 ± 20.8	44.3 ± 9.4	20.3 ± 14.3
20	141.8 ± 29.1	44.8 ± 1.8	86.9 ± 0.4	47.1 ± 3.7*
30	29.8 ± 13.9	19.7 ± 10.7	50.6 ± 17.9	23.3 ± 18.7

Nitrogenase activity of intact filaments was measured with cell suspensions incubated for 24 and 72 h in nitrate-free medium $BG11_0$. The filaments were incubated with different O_2 (0 to 30%) and N_2 (80 to 50%) concentrations in the presence of 20% acetylene for 2 h. Data represent mean and SD of at least three individual experiments. Statistically significant differences from the wild type are indicated by asterisks ($P < 0.05$). Chla, chlorophyll *a*.

sativum), spinach, or *Mesostigma viride* (Kerr and Groves, 1975; Macheroux et al., 1992; Iwamoto and Ikawa, 2000) and significantly higher than that of At-GOX2. These enzyme kinetics data support the notion that the cyanobacterial GOX-like proteins emerged from ancestral LOX proteins. In the anoxic Precambrian ocean, fermentation was the dominant metabolic mode (Barnabas et al., 1982), and these LOX proteins were likely involved in the utilization of the available fermentation product L-lactate as observed in extant anaerobic microbial mats (Anderson et al., 1987). Apparently, during the evolution of plant GOX, the efficiency of glycolate oxidation was greatly improved, while the efficiency of L-lactate oxidation was strongly decreased.

To mimic some of the alterations that were responsible for the change of L-lactate to glycolate preference, we performed a mutational analysis of No-LOX, using published information on the structure of the active sites of the GOX and LOX enzymes from other organisms (for example, Stenberg and Lindqvist, 1997). To this end, the amino acids at positions 82, 112, and 212 from No-LOX were exchanged for the corresponding amino acids in plant GOX. Activity measurements with glycolate and L-lactate as substrates revealed that all three positions affect the relative substrate preference of No-LOX. The individual or combined exchanges at positions 82 and 212 all improved the reactivities of the respective No-LOX variants with glycolate and, with the exception of the M82T mutation, decreased their reactivities with L-lactate. The combination of these two mutations in a double mutant resulted in a 10-fold higher GOX activity and a 15-fold lower LOX/GOX ratio. These results suggest that the No-LOX active site is optimized for the use of L-lactate as a substrate. The F212V variant shows that the exchange of one amino acid is capable of inducing threefold higher activity levels with glycolate and 10-fold lower activity levels with L-lactate, representing a threefold enhanced performance, compared with Cr-LOX. In the triple-substituted No-LOX variant, the LOX/GOX activity ratio was close to that of the plant enzyme. However, the maximum GOX activity (0.6 ± 0.1 μmol min^{-1} mg^{-1} in L112W/F212V) achieved by these alterations in No-LOX was still 40 times lower than that of At-GOX2, indicating that a number of additional mutations and corresponding fine adjustments must have contributed to the evolution of specific GOX enzymes in land plants.

Compared with land plants, the overall photorespiratory production of glycolate is much lower in cyanobacteria and green algae due to the presence of CCMs in these organisms (Giordano et al., 2005; Huege et al., 2011). It appears that the low glycolate synthesis rate in cyanobacteria and the relatively high affinity of No-LOX for glycolate (eightfold lower K_m in comparison with At-GOX2) was essential for the successful complementation of the HCR phenotype of the Δ*glcD1/D2 Synechocystis* double mutant. However, the very low GOX activities of the proteins from *Nostoc* and *Chlamydomonas* indicate that these enzymes are unlikely to be involved in photorespiratory metabolism. Instead, our analysis of the *Nostoc* Δ*lox* mutant supports earlier studies, suggesting that GlcDs (in *Nostoc* encoded by *alr*5269 - *glcD1* and *all*4443 - *glcD2*) are responsible for the photorespiratory glycolate-to-glyoxylate conversion in cyanobacteria and green algae (Marek and Spalding, 1991; Nakamura et al., 2005; Eisenhut et al., 2008a). The *Chlamydomonas* GlcD seems to be located in the mitochondrion and not in the peroxisomes, which is where the GOX of land plants is confined (Atteia et al., 2009) and probably where Cr-LOX is also confined (Shinozaki et al., 2009). Interestingly, a GlcD-like enzyme is present in the mitochondria of land plants too (Bari et al., 2004); however, this enzyme shows only low activity with glycolate and prefers D-lactate, indicating that it is unlikely to contribute to photorespiration (Engqvist et al., 2009).

As mentioned above, our BLASTP searches with the translated genomes of cyanobacteria revealed that GOX-like proteins are exclusively present in cyanobacteria capable of N_2 fixation. These species included heterocystous (e.g., *Nostoc*), filamentous nonheterocystous (e.g., *Trichodesmium* sp), and unicellular (e.g., *Cyanothece* spp) cyanobacteria that represent separate clades within the cyanobacterial radiation (Gupta and Mathews, 2010). Available data indicate that all ancient cyanobacteria were capable of fixing N_2 until O_2 accumulated in the environment ~2.5 billion years ago (Hartmann and Barnum, 2010). As a consequence of O_2 accumulation, and the almost simultaneous increase in nitrate levels, many cyanobacteria may have lost the ability to grow diazotrophically because they were unable to maintain nitrogenase activity in the presence of O_2 (Falkowski, 1997; Berman-Frank et al., 2003). Since the inactivation of nitrogenase by O_2 represents the main obstacle for N_2 fixation, cyanobacteria have evolved several elaborate O_2 protection strategies, including mechanisms to scavenge any environmental O_2 that diffuses with N_2 (Fay, 1992; Berman-Frank et al., 2003; Walsby, 2007). Respiration is one of these nitrogenase-protecting mechanisms. It was shown that mutants of *Nostoc* defective in terminal oxidases were not only affected in respiration but also lost their capability for diazotrophic growth (Valladares et al., 2003, 2007). In addition, respiration is necessary to provide the N_2 fixation processes with ATP and reductants in the absence of light (Fay, 1992). On the other hand, sugar catabolism in the anoxic heterocyst could well include anaerobic glycolysis to L-lactate, which is converted back to pyruvate by No-LOX. Because this process consumes O_2, it could assist in protecting nitrogenase.

The absence of No-LOX did not impair the growth of the corresponding *Nostoc* mutant, Δ*lox*, in normal photorespiratory

conditions with nitrate-containing medium. However, the mutant was unable to grow diazotrophically, indicating that No-LOX contributes to N_2 fixation in *Nostoc*, possibly by scavenging O_2 from the heterocysts. This suggestion is based on two central experiments summarized in Figure 5 and Table 4. First, in contrast with wild-type *Nostoc*, the mutant Δ*lox* is unable to grow without combined N sources in air but grows under microaerobic conditions. Second, nitrogenase activity of the Δ*lox* reached maximal levels under microaerobic conditions and was inhibited by increasing O_2 concentrations, whereas the wild type showed optimum nitrogenase activity at 20% O_2 (Table 4). The lower nitrogenase activities detected at low O_2 concentrations in *Nostoc* wild type is probably related to the essential role of respiration in the supply of energy to nitrogenase. The unicellular *Crocosphaera watsonii* also showed maximal N_2 fixation in the presence of oxygen (5% O_2), whereas anoxic conditions completely abolished nitrogenase activity (Compaoré and Stal, 2010). Although not fully identical, the oxygen sensitivity of the Δ*lox* mutant is similar to that of a *Nostoc* mutant in which the two N-regulated terminal respiratory oxidases were deleted, resulting in a complete loss of nitrogenase activity (Valladares et al., 2003, 2007). Interestingly, the affinity of No-LOX for the cosubstrate O_2 was in the same range as cyanobacterial respiratory cytochrome oxidases (Jensen and Cox, 1983; Pils and Schmetterer, 2001) and would be sufficient to decrease the O_2 content inside heterocysts below levels toxic for nitrogenase. However, in Δ*lox*, nitrogenase was only partially inactivated under comparable conditions, even after the incubation of the filaments in air for 72 h.

In addition to the O_2-scavenging function, No-LOX could also be important for the redirection of lactate originating from anaerobic glycolysis into gluconeogenesis, similar to the well-known Cori cycle of mammals. The energy requirements of this process would then suggest the cooperation of the heterocysts with the photosynthetic cells of *Nostoc*. In both cases, the generated H_2O_2 could be removed by rubredoxin-like proteins, such as RbrA. These proteins use H_2 as a reducing agent, which is produced as a byproduct of N_2 fixation (Zhao et al., 2007). Our current hypothesis, that No-LOX represents one of several oxygen-scavenging mechanisms in *Nostoc*, needs additional support by more data.

In summary, it appears that cyanobacteria that maintained their capacity for N_2 fixation also kept the oxygen-consuming enzyme LOX as one of the mechanisms to protect nitrogenase from O_2 inactivation. Conversely, the loss of nitrogenase was accompanied by the loss of *lox* genes. Whether this indicates that the primary endosymbiont was still able to fix N_2, a capability which was later lost, cannot be determined from our data. Our data also suggest that the enzyme acquired its specificity for glycolate and became the photorespiratory GOX sometime after the last common ancestor of *Chlamydomonas* and land plants.

METHODS

Strains and Culture Conditions

The Glc-tolerant wild-type strain *Synechocystis* sp PCC 6803 was obtained from N. Murata (National Institute for Basic Biology, Okazaki, Japan). *Nostoc* (*Anabaena*) sp PCC 7120 wild type was obtained from the Pasteur Culture Collection (Paris). The *Chlamydomonas reinhardtii* strain 137c *mt*$^+$ was obtained from Y. Tsubo (Kobe University, Hyogo, Japan) via H. Takeda (Niigata University, Niigata, Japan).

The construction of the *Synechocystis* single mutants Δ*glcD1* (*sll*0404::Km) and Δ*glcD2* (*slr*0806::Sp) and the double mutant Δ*glcD1/D2* was previously described (Eisenhut et al., 2006, 2008a). Axenic cultures were grown on Petri dishes at 30°C under constant illumination of 30 μmol photons m^{-2} s^{-1} (warm white light; Osram L58 W32/3) using agar-solidified BG11 medium (Rippka et al., 1979) buffered to pH 8.0 with 20 mM TES-KOH. Transformants were initially selected on media containing one of the following: 10 mg L^{-1} kanamycin (Km), 4 mg L^{-1} Sp, or 5 mg L^{-1} chloramphenicol (Cm). The segregation of clones and cultivation of mutants were done with one of the following: 50 mg L^{-1} Km, 20 mg L^{-1} Sp, or 5 mg L^{-1} Cm. All strains are listed in the Supplemental Table 1 online.

For the physiological characterization of *Synechocystis* mutants, axenic cultures of a defined optical density at 750 nm (OD_{750}) of 0.8 were grown photoautotrophically in batch cultures at 29°C under continuous illumination of 100 μmol photons m^{-2} s^{-1} (warm white light; Osram L58 W32/3) and bubbled with air enriched with CO_2 (5%, defined as high inorganic carbon [HC]) in BG11 medium at pH 8.0 or bubbled with air (0.035% CO_2, defined as low inorganic carbon [LC]) in BG11 medium at pH 7.0.

For the physiological characterization of *Nostoc* mutants, axenic cultures of an OD_{750} 1.2 were grown photoautotrophically in batch cultures at 29°C under continuous illumination of 40 μmol photons m^{-2} s^{-1} at HC in standard BG11 medium containing nitrate as combined N source or in nitrate-free BG11 medium ($BG11_0$) at pH 8.0. To grow *Nostoc* under microaerobic conditions, the cells were bubbled with N_2 in $BG11_0$ supplemented with 10 mM $NaHCO_3$.

For the cloning of the *lox* cDNA from *C. reinhardtii*, the wild-type strain (137c *mt*$^+$) was grown photoautotrophically with 500 mL of HS medium (Sueoka, 1960) under continuous illumination of 200 μmol photons m^{-2} s^{-1} at 25°C. The culture was bubbled with ambient air (LC) at a rate of 200 mL min^{-1}.

Growth was monitored by measurements of the OD_{750}. Photosynthetic pigment concentrations were estimated as described by Huckauf et al. (2000). Contamination by heterotrophic bacteria was checked by spreading of 0.2 mL of culture on Luria-Bertani plates.

DNA Manipulation and Generation of Protein Expression Strains or Mutants

Total DNA from *Synechocystis* and *Nostoc* was isolated according to Hagemann et al. (1997). All other DNA techniques, such as plasmid isolation, transformation of *Escherichia coli*, ligations, and restriction analysis (restriction enzymes were obtained from Fermentas or New England Biolabs), were standard methods.

To generate overexpressing strains of *E. coli* as well as of *Synechocystis*, we amplified the coding sequences of the selected genes by PCR using DNA of *Nostoc* or cDNA of *Arabidopsis thaliana* as templates, gene-specific primers with added appropriate cleavage sites (see Supplemental Table 2 online), and proofreading Elongase enzyme (Invitrogen).

For the cloning of the *C. reinhardtii lox* cDNA, mRNA was isolated from wild-type cells in exponential growth phase using RNAgents Total RNA isolation system (Promega) and PolyATract mRNA isolation system (Promega). One microgram of mRNA was reverse transcribed using PowerScript reverse transcriptase (Clontech) with a gene-specific primer (CrLOX_R1; see Supplemental Table 2 online). The resulting cDNA solution was diluted (1:10) with TE buffer and then used as template for PCR amplification. A cDNA fragment containing LOX coding region was amplified using PrimeSTAR GXL DNA polymerase (TaKaRa BIO) with a primer pair of CrLOX_F1 and CrLOX_R2 (see Supplemental Table 2 online). The amplified fragment was then cloned into the pGEMT-easy

vector (Promega) and sequenced with a BigDye Terminator version 3.1 cycle sequence kit (Applied Biosystems).

Site-specific mutants of No-LOX (All0170) were generated by PCR with Phusion high-fidelity polymerase using phosphorylated mutagenesis primers (see Supplemental Table 2 online) and the cloned wild-type *all*0170 gene as template. First, single amino acid exchanges at the positions 82, 112, or 212 of No-LOX were introduced. Second, double amino acid exchanges were made using the single-mutant constructs as template, and finally the triple amino acid exchange was obtained using the double mutant construct (M82T/L112W). The site-specific mutagenesis constructs were self-ligated and transformed into *E. coli*. All constructs were verified by restriction and sequence analyses.

For expression of the genes from *Nostoc* (No-LOX, *lox*, *all*0170), *Arabidopsis* (At-GOX2, At3g14415), *C. reinhardtii* (Cr-LOX, XP_001703481; AB610509), and the site-specific mutants of No-LOX in *E. coli*, the verified coding sequences were transferred into the expression vector pET-28a (Novagen) using *Nde*I/*Eco*RI for No-LOX, Cr-LOX, and the site-specific No-LOX mutants and *Bam*HI/*Sal*I for At-GOX2, respectively (see Supplemental Table 2 online). The verified recombinant pET-28a vectors were transformed into *E. coli* strain BL21 DE3.

For expression of No-LOX and At-GOX2 in the Δ*glcD1/D2* double mutant of *Synechocystis*, the coding sequences were transferred into the expression vector pAII downstream of the *psba2* promoter (Lagarde et al., 2000) using *Nde*I/*Kpn*I (see Supplemental Table 2 online). For clone selection, the Cm resistance cartridge from pCAT was cloned into pAII downstream of the *psba2* promoter and the inserted genes using the *Bam*HI cleavage site. The generated plasmids were transformed into the HC-requiring Δ*glcD1/D2* double mutant of *Synechocystis* (Eisenhut et al., 2008a). Transformants were selected on agar plates supplemented with Cm at LC conditions.

To generate the *Nostoc* mutant Δ*lox* (Δ*all*0170::Sp), a 975-bp fragment of the upstream region and a 898-bp fragment of the downstream region of the gene *all*0170 were amplified using specific primers with cleavage sites for *Xho*I/*Bam*HI and *Bam*HI/*Sac*I, respectively (see Supplemental Table 2 online). The upstream region was cloned into pDrive (Qiagen) using *Xho*I and *Apa*I generating pDrive-*all*0170-up. Subsequently, the downstream region was cloned into pDrive-*all*0170-up after cleavage with *Apa*I and *Sac*I. The adjacent regions of *all*0170 were cloned into the cargo plasmid pRL271 (kindly provided by W. Lockau, Humboldt University Berlin, Germany) using *Xho*I and *Sac*I. The cargo plasmid pRL271 is a cloning vector for *sacB*-mediated positive selection of targeted gene replacement and double recombinants in cyanobacteria (Black et al., 1993). Finally, the Sp resistance cartridge from pAII::Sp was cloned between the *all*0170 up- and downstream regions to generate pRL271-*all*0170::Sp using *Bam*HI cleavage sites (see Supplemental Figure 3 online). The verified construct was conjugated into *Nostoc* as previously described (Cai and Wolk, 1990). Double recombinant filaments were selected on agar plates supplemented with Sp and/or Suc.

Purification of Recombinant GOX Proteins after Overexpression in *E. coli*

E. coli BL21 strains containing pET-28a-NoLOX or site-specific No-LOX mutagenesis constructs, pET-28a-CrLOX, and pET28a-AtGOX2 were grown in Luria-Bertani medium to an OD_{750} of 0.6. Gene expression was induced by addition of 1 mM isopropyl β-1-D-thiogalactopyranoside for 16 h at 30°C. The fusion proteins were purified via their N-terminal His-tags using Ni-NTA Sepharose according to the protocol of the supplier (Invitrogen). The cells were harvested and resuspended in 20 mM Tris-HCl, pH 8.0, containing 500 mM NaCl, 1 mM DTT, and 0.1 mM FMN. Protein was extracted by ultrasonic treatments (2 × 60 s, 90 W) in ice. Soluble protein extracts were used for affinity chromatography on Ni-NTA Sepharose using 20 mM Tris-HCl, pH 8.0, containing 500 mM NaCl, 1 mM DTT, and 0.1 mM FMN supplemented with 40 up to 80 mM imidazole as washing buffers. The same buffer supplemented with 200 mM imidazole was used as elution buffer. The eluted proteins were combined and desalted using PD-10 columns (GE Healthcare). Finally, the recombinant enzymes were dissolved in 20 mM Tris-HCl, pH 8.0, with 1 mM DTT and 0.1 mM FMN. The eluted proteins were checked regarding purity using SDS-PAGE and staining by Coomassie Brilliant Blue (see Supplemental Figure 2 online) and subsequently used for enzyme measurements and antibody production.

Enzyme Measurements

Enzyme activity was measured in 100 mM Tris-HCl, pH 8.0, containing 5 mM $MgCl_2$, 0.5 mM EDTA, 1 mM DTT, 0.1 mM FMN, and 0.0083% Triton-X 100 at 30°C. The O_2 consumption of LOX and GOX was assayed using Hansatech oxygen electrodes (Oxygraph). The assay was started by adding of different substrates after 3 min of equilibration. One unit of enzyme activity was defined by the formation of 1 μmol of O_2 in 1 min at 30°C. The affinity of No-LOX for oxygen was estimated according to the methods of Macheroux et al. (1993) and Mills et al. (2001) using different L-lactate concentrations (1 to 10 mM) and different enzyme amounts. Additionally, hydrogen peroxide production was measured using 3,3′,5,5′-tetramethylbenzidine according to Josephy et al. (1982) and Kireyko et al. (2006). The recombinant proteins were incubated for 5 min without (control) or 1 mM substrate in the enzyme buffer described above. H_2O_2 was quantified by adding 2 mM 3,3′,5,5′-tetramethylbenzidine and 2 units of horseradish peroxidase. Kinetic parameters were calculated by nonlinear regression fit to the Michaelis-Menten equation (Sigma Plot software) or by linear regression analysis of the double-reciprocal data pairs (Lineweaver-Burk).

Immunoblotting and Antibody Purification

Polyclonal antibodies specific for No-LOX or At-GOX2 were raised in rabbits using the corresponding pure recombinant proteins as antigens (Seqlab). To increase the specificity of the antibodies, they were purified as follows. About 1 mg of recombinant protein was separated on 12% acrylamide gels and blotted onto nylon membranes (GE Healthcare). After visualization by Ponceau S staining (0.2% Ponceau S in 0.25% acetic acid), the respective bands were cut and the membrane pieces were washed in glycine buffer (100 mM glycine-HCl, pH 2.5) for 5 min. After washing, the membranes were blocked with 3% BSA for 60 min and incubated with the antisera after threefold dilution in PBS overnight at 4°C while shaking. After washing with PBS, the antibodies were eluted with 1 mL glycine buffer for 10 min. The elution was repeated and the fractions were pooled. To adjust the pH at ~7.0, 200 μL of 1 M Tris-HCl, pH 8.0, was added to the purified antibody solutions, and BSA (1 mg mL^{-1}) was added as stabilizer.

For immunoblotting, 20 mL of a culture of *Synechocystis* grown for 24 h under HC or LC conditions was harvested by centrifugation (3140 rcf, 4°C, 10 min). The cell pellet was immediately frozen and stored at −80°C. Total proteins were extracted by sonication in ice-cold 10 mM HEPES-NaOH, pH 7.5, containing phenylmethylsulfonyl fluoride. Equal amounts of soluble protein (10 μg) were separated by PAGE (12% polyacrylamide) and subsequently blotted onto polyvinylidene fluoride membranes (Bio-Rad). The cross-reacting bands were detected by the purified No-LOX- or At-GOX2-antibodies (diluted 400- or 1000-fold) using horseradish peroxidase–conjugated anti-rabbit IgG (Bio-Rad) as secondary antibody.

Quantification of Glycolate

Glycolate was determined using a metabolite targeted and quantitatively standardized extended variant of the previously established gas chromatography–electron impact–time of flight–mass spectrometry profiling analysis. Cells grown in liquid media at HC or LC conditions were

harvested by fast filtration in the light and were immediately frozen in liquid N_2. The whole procedure has been described in detail previously (Eisenhut et al., 2008b; Huege et al., 2011), but instead of MSTFA as derivatization agent, TBDMS was used.

Nitrogenase Activity Measurements

Cultures of *Nostoc* wild type or Δ*lox* mutant were shaken in 300-mL Erlenmeyer flasks at 29°C under continuous illumination (40 μmol photons m^{-2} s^{-1}) in $BG11_0$ at pH 8.0 in air (LC). Two milliliters of culture were placed in a 10-mL vial sealed with a rubber stopper and bubbled for 5 min with different ratios of O_2 and N_2 to achieve defined O_2 concentrations in the presence of 20% (v/v) acetylene using a gas-mixing system of mass flow controllers (Brooks 5850S) and control unit (Brooks 0152) as described earlier (Staal et al., 2001). After 2 h of incubation under the growth conditions, ethylene was measured in the head space of the vial using gas chromatography (Chrompack CP9001) equipped with a flame ionization detector (FID) and a wide-bore silica-fused (0.53-mm internal diameter) Porapak U column (Chrompack). The carrier gas was N_2 at 10 mL min^{-1}, and the flows of H_2 and air for the flame ionization detector were 30 and 300 mL min^{-1}, respectively. The temperatures for injector, detector, and oven were 90, 120, and 55°C, respectively.

All experiments (growth rates of different strains, enzyme activity measurements, and metabolite contents) were repeated at least three time using independent biological replicates. Statistically significant differences estimated using Student's *t* test.

Phylogenetic Analysis of GOXs and GOX-Like Proteins

To analyze the evolutionary history of the GOX enzymes in the plant 2PG metabolism, proteins similar to the *Arabidopsis* GOX2 (At3g14415; extracted from The Arabidopsis Information Resource database: http://www.Arabidopsis.org/) were searched by the BLASTP (Altschul and Lipman, 1990) algorithm. Among cyanobacteria, the gene *all*0170 from *Nostoc* was identified to encode for a GOX-like protein (CyanoBase: http://genome.kazusa.or.jp/cyanobase/). Subsequently, this protein sequence was used for further searches. The sequences were retrieved from the following databases: (1) GenBank (http://www.ncbi.nlm.nih.gov/genbank/), (2) PlantGDB (http://www.plantgdb.org/OsGDB/), (3) CyanoBase (http://genome.kazusa.or.jp/cyanobase), (4) *Cyanidioschyzon merolae* genome browser (http://merolae.biol.s.u-tokyo.ac.jp/; Matsuzaki et al., 2004), and (5) The Arabidopsis Information Resource (http://www.Arabidopsis.org/). For phylogenetic analyses, the homologous amino acid sequences were aligned using the ClustalW algorithm (Thompson et al., 1994) integrated in the BioEdit Sequence alignment editor (Hall, 1999). The alignment is available as Supplemental Data Set 1 online. The neighbor-joining tree of putative and biochemically characterized LOX or GOX proteins was inferred using MEGA version 4.0 (Tamura et al., 2007). The Jones-Taylor-Thornton substitution model (Jones et al., 1992) was selected assuming a gamma correction for heterogeneity across sites. Reliability for internal branch was assessed using the bootstrapping method (1000 bootstrap replicates). Graphical representation and edition of the phylogenetic tree were performed with TreeDyn (v198.3) (Chevenet et al., 2006).

Accession Numbers

Sequence data from this article can be found in the Arabidopsis Genome Initiative or GenBank/EMBL/CyanBase/DDBJ databases under the following accession numbers: *Arabidopsis* GOX2 (At3g14415), *Arabidopsis* HAOX1 (At3g14130), *Zea mays (*ACN28768), *Vitis vinifera* (CAN67413), *Spinacia oleracea* (AAA34030), *Physcomitrella patens* (XP_001769086), *C. reinhardtii* CC-503 (XP_001703481, AB610509), *Volvox carteri* (XP_002946783), *Ectocarpus siliculosus* (CBN74053), *Cyanothece* sp PCC 7822 (YP_003890366), *Salmonella enterica* strain GA-MM04042433 (ZP_03218859), *Acidaminococcus* sp D21 (ZP_039818), *Lactococcus lactis* Il1403 (AAK05350), *Weissella paramesenteroides* ATCC33313 (ZP_04782696), *Aerococcus viridans* IF012219 (BAA09172), *Enterococus faecium* DO (ZP_05714515), *Oryza sativa* (Os07g0152900), *Anabaena variabilis* ATCC 29413 (Ava_1430), *Nostoc punctiforme* ATCC 29133 (Npun_R5717), *Trichodesmium erythraeum* IMS101 (Tery_2398), *Cyanothece* sp ATCC 51,142 (cce_1717), and *Cyanidioschyzon merolae* 10D (CMQ436C).

Supplemental Data

The following materials are available in the online version of this article.

Supplemental Figure 1. Amino Acid Sequence Alignment of GOX and LOX.

Supplemental Figure 2. Purification of Recombinant Proteins.

Supplemental Figure 3. Genotypic Characterization of the *Nostoc* Mutant Δ*lox*.

Supplemental Table 1. Strains Used in this Work.

Supplemental Table 2. Primers Used in this Work.

Supplemental Data Set 1. Text File of the Alignment Used for the Phylogenetic Analysis Shown in Figure 1.

ACKNOWLEDGMENTS

The excellent technical assistance of Manja Henneberg, Kathrin Jahnke, and Klaudia Michl is greatly acknowledged. The generous help of Wolfgang Lockau and his group in establishing genetics with *Nostoc* 7120 is highly appreciated. The work was supported by a grant from the Deutsche Forschungsgemeinschaft to M.H. and the Forschergruppe FOR 1186-Promics.

AUTHOR CONTRIBUTIONS

M.H. designed research. C.H., R.K., J.H., Y.T., and L.J.S., performed research. C.H., R.K., J.H., L.J.S., Y.T., J.K., Y.S., H.B., and M.H. analyzed data. C.H., R.K., L.J.S., J.K., Y.S., H.B., and M.H. wrote the article.

Received June 8, 2011; revised July 15, 2011; accepted July 19, 2011; published August 9, 2011.

REFERENCES

Altschul, S.F., and Lipman, D.J. (1990). Protein database searches for multiple alignments. Proc. Natl. Acad. Sci. USA **87:** 5509–5513.

Anderson, K.L., Tayne, T.A., and Ward, D.M. (1987). Formation and fate of fermentation products in hot spring cyanobacterial mats. Appl. Environ. Microbiol. **53:** 2343–2352.

Atteia, A., et al. (2009). A proteomic survey of *Chlamydomonas reinhardtii* mitochondria sheds new light on the metabolic plasticity of the organelle and on the nature of the α-proteobacterial mitochondrial ancestor. Mol. Biol. Evol. **26:** 1533–1548.

Badger, M.R., Price, G.D., Long, B.M., and Woodger, F.J. (2006). The environmental plasticity and ecological genomics of the cyanobacterial CO_2 concentrating mechanism. J. Exp. Bot. **57:** 249–265.

Bari, R., Kebeish, R., Kalamajka, R., Rademacher, T., and Peterhänsel, C. (2004). A glycolate dehydrogenase in the mitochondria of *Arabidopsis thaliana*. J. Exp. Bot. **55:** 623–630.

Barnabas, J., Schwartz, R.M., and Dayhoff, M.O. (1982). Evolution of major metabolic innovations in the precambrian. Orig. Life **12:** 81–91.

Bauwe, H., Hagemann, M., and Fernie, A.R. (2010). Photorespiration: Players, partners and origin. Trends Plant Sci. **15:** 330–336.

Beezley, B.B., Gruber, P.J., and Frederick, S.E. (1976). Cytochemical localization of glycolate dehydrogenase in mitochondria of *Chlamydomonas*. Plant Physiol. **58:** 315–319.

Berman-Frank, I., Lundgren, P., and Falkowski, P. (2003). Nitrogen fixation and photosynthetic oxygen evolution in cyanobacteria. Res. Microbiol. **154:** 157–164.

Black, T.A., Cai, Y.P., and Wolk, C.P. (1993). Spatial expression and autoregulation of *hetR*, a gene involved in the control of heterocyst development in *Anabaena*. Mol. Microbiol. **9:** 77–84.

Blackwell, R.D., Murray, A.J.S., Lea, P.J., Kendall, A., Hall, N.P., Turner, J.C., and Wallsgrove, R.M. (1988). The value of mutants unable to carry out photorespiration. Photosynth. Res. **16:** 155–176.

Cai, Y.P., and Wolk, C.P. (1990). Use of a conditionally lethal gene in *Anabaena* sp. strain PCC 7120 to select for double recombinants and to entrap insertion sequences. J. Bacteriol. **172:** 3138–3145.

Chauvin, L., Tural, B., and Moroney, J.V. (2008). *Chlamydomonas reinhardtii* has genes for both glycolate oxidase and glycolate dehydrogenase. In Photosynthesis. Energy from the Sun: 14th International Conference of Photosynthesis, J.F. Allen, E. Gantt, J.H. Golbeck, and C.B. Osmond, eds (Dordrecht, The Netherlands: Springer), pp. 823–827.

Chevenet, F., Brun, C., Bañuls, A.L., Jacq, B., and Christen, R. (2006). TreeDyn: Towards dynamic graphics and annotations for analyses of trees. BMC Bioinformatics **7:** 439–448.

Clagett, C.O., Tolbert, N.E., and Burris, R.H. (1949). Oxidation of α-hydroxy acids by enzymes from plants. J. Biol. Chem. **178:** 977–987.

Codd, G.A., Lord, J.M., and Merrett, M.J. (1969). The glycollate oxidising enzyme of algae. FEBS Lett. **5:** 341–342.

Colman, B. (1989). Photosynthetic carbon assimilation and the suppression of photorespiration in the cyanobacteria. Aquat. Bot. **34:** 211–231.

Compaoré, J., and Stal, L.J. (2010). Oxygen and the light-dark cycle of nitrogenase activity in two unicellular cyanobacteria. Environ. Microbiol. **12:** 54–62.

Deusch, O., Landan, G., Roettger, M., Gruenheit, N., Kowallik, K.V., Allen, J.F., Martin, W., and Dagan, T. (2008). Genes of cyanobacterial origin in plant nuclear genomes point to a heterocyst-forming plastid ancestor. Mol. Biol. Evol. **25:** 748–761.

Eisenhut, M., Huege, J., Schwarz, D., Bauwe, H., Kopka, J., and Hagemann, M. (2008b). Metabolome phenotyping of inorganic carbon limitation in cells of the wild type and photorespiratory mutants of the cyanobacterium *Synechocystis* sp. strain PCC 6803. Plant Physiol. **148:** 2109–2120.

Eisenhut, M., Ruth, W., Haimovich, M., Bauwe, H., Kaplan, A., and Hagemann, M. (2008a). The photorespiratory glycolate metabolism is essential for cyanobacteria and might have been conveyed endosymbiontically to plants. Proc. Natl. Acad. Sci. USA **105:** 17199–17204.

Eisenhut, M., Kahlon, S., Hasse, D., Ewald, R., Lieman-Hurwitz, J., Ogawa, T., Ruth, W., Bauwe, H., Kaplan, A., and Hagemann, M. (2006). The plant-like C2 glycolate cycle and the bacterial-like glycerate pathway cooperate in phosphoglycolate metabolism in cyanobacteria. Plant Physiol. **142:** 333–342.

Engqvist, M., Drincovich, M.F., Flügge, U.I., and Maurino, V.G. (2009). Two D-2-hydroxy-acid dehydrogenases in *Arabidopsis thaliana* with catalytic capacities to participate in the last reactions of the methylglyoxal and β-oxidation pathways. J. Biol. Chem. **284:** 25026–25037.

Eprintsev, A.T., Semenov, A.E., Navid, M., and Popov, V.N. (2009). Physical, chemical, and regulatory properties of glycolate oxidase in C-3 and C-4 plants. Russ. J. Plant Physiol. **56:** 164–167.

Falkowski, P.G. (1997). Evolution of the nitrogen cycle and its influence on the biological sequestration of CO_2 in the ocean. Nature **387:** 272–275.

Fay, P. (1992). Oxygen relations of nitrogen fixation in cyanobacteria. Microbiol. Rev. **56:** 340–373.

Frederick, S.E., Gruber, P.J., and Tolbert, N.E. (1973). The occurence of glycolate dehydrogenase and glycolate oxidase in green plants: An evolutionary survey. Plant Physiol. **52:** 318–323.

Giordano, M., Beardall, J., and Raven, J.A. (2005). CO_2 concentrating mechanisms in algae: Mechanisms, environmental modulation, and evolution. Annu. Rev. Plant Biol. **56:** 99–131.

Gupta, R.S., and Mathews, D.W. (2010). Signature proteins for the major clades of Cyanobacteria. BMC Evol. Biol. **10:** 24.

Hagemann, M., Schoor, A., Jeanjean, R., Zuther, E., and Joset, F. (1997). The stpA gene form synechocystis sp. strain PCC 6803 encodes the glucosylglycerol-phosphate phosphatase involved in cyanobacterial osmotic response to salt shock. J. Bacteriol. **179:** 1727–1733.

Hall, T.A. (1999). BioEdit: A user-friendly biological sequence alignment editor and analysis program for Windows 95/98/NT. Nucleic Acids Symp. Ser. **41:** 95–98.

Hartmann, L.S., and Barnum, S.R. (2010). Inferring the evolutionary history of Mo-dependent nitrogen fixation from phylogenetic studies of *nifK* and *nifDK*. J. Mol. Evol. **71:** 70–85.

Huckauf, J., Nomura, C., Forchhammer, K., and Hagemann, M. (2000). Stress responses of *Synechocystis* sp. strain PCC 6803 mutants impaired in genes encoding putative alternative sigma factors. Microbiology **146:** 2877–2889.

Huege, J., Goetze, J., Schwarz, D., Bauwe, H., Hagemann, M., and Kopka, J. (2011). Modulation of the major paths of carbon in photorespiratory mutants of *synechocystis*. PLoS ONE **6:** e16278.

Husic, D.W., Husic, H.D., and Tolbert, N.E. (1987). The oxidative photosynthetic carbon cycle or C_2 cycle. Crit. Rev. Plant Sci. **5:** 45–100.

Iwamoto, K., and Ikawa, T. (2000). A novel glycolate oxidase requiring flavin mononucleotide as the cofactor in the prasinophycean alga *Mesostigma viride*. Plant Cell Physiol. **41:** 988–991.

Jensen, B.B., and Cox, R.P. (1983). Effect of oxygen concentration on dark nitrogen fixation and respiration in cyanobacteria. Arch. Microbiol. **135:** 287–292.

Jones, D.T., Taylor, W.R., and Thornton, J.M. (1992). The rapid generation of mutation data matrices from protein sequences. Comput. Appl. Biosci. **8:** 275–282.

Josephy, P.D., Eling, T., and Mason, R.P. (1982). The horseradish peroxidase-catalyzed oxidation of 3,5,3′,5′-tetramethylbenzidine. Free radical and charge-transfer complex intermediates. J. Biol. Chem. **257:** 3669–3675.

Kaplan, A., and Reinhold, L. (1999). CO_2 concentrating mechanisms in photosynthetic microorganisms. Annu. Rev. Plant Physiol. Plant Mol. Biol. **50:** 539–570.

Kern, R., Bauwe, H., and Hagemann, M. (2011). Evolution of enzymes involved in the photorespiratory 2-phosphoglycolate cycle from cyanobacteria via algae toward plants. Photosynth. Res., in press.

Kerr, M.W., and Groves, D. (1975). Purification and properties of glycollate oxidase from *Pisum sativum* leaves. Phytochemistry **14:** 359–362.

Kireyko, A.V., Veselova, I.A., and Shekhovtsova, T.N. (2006). Mechanisms of peroxidase oxidation of o-dianisidine, 3,3′,5,5′-tetramethylbenzidine, and o-phenylenediamine in the presence of sodium dodecyl sulfate. Russ. J. Bioorganic Chem. **32:** 71–77.

Kumar, K., Mella-Herrera, R.A., and Golden, J.W. (2010). Cyanobacterial heterocysts. Cold Spring Harb. Perspect. Biol. **2:** a000315.

Lagarde, D., Beuf, L., and Vermaas, W. (2000). Increased production of zeaxanthin and other pigments by application of genetic engineering techniques to *Synechocystis* sp. strain PCC 6803. Appl. Environ. Microbiol. **66:** 64–72.

Leiros, I., Wang, E., Rasmussen, T., Oksanen, E., Repo, H., Petersen, S.B., Heikinheimo, P., and Hough, E. (2006). The 2.1 A structure of *Aerococcus viridans* L-lactate oxidase (LOX). Acta Crystallogr. Sect. F Struct. Biol. Cryst. Commun. **62:** 1185–1190.

Lindqvist, Y. (1989). Refined structure of spinach glycolate oxidase at 2 A resolution. J. Mol. Biol. **209:** 151–166.

Lindqvist, Y., and Brändén, C.I. (1989). The active site of spinach glycolate oxidase. J. Biol. Chem. **264:** 3624–3628.

Macheroux, P., Kieweg, V., Massey, V., Söderlind, E., Stenberg, K., and Lindqvist, Y. (1993). Role of tyrosine 129 in the active site of spinach glycolate oxidase. Eur. J. Biochem. **213:** 1047–1054.

Macheroux, P., Mulrooney, S.B., Williams, C.H., Jr., and Massey, V. (1992). Direct expression of active spinach glycolate oxidase in *Escherichia coli*. Biochim. Biophys. Acta **1132:** 11–16.

Maeda-Yorita, K., Aki, K., Sagai, H., Misaki, H., and Massey, V. (1995). L-lactate oxidase and L-lactate monooxygenase: Mechanistic variations on a common structural theme. Biochimie **77:** 631–642.

Marek, L.F., and Spalding, M.H. (1991). Changes in photorespiratory enzyme activity in response to limiting CO_2 in *Chlamydomonas reinhardtii*. Plant Physiol. **97:** 420–425.

Margulis, L. (1970). Origin of Eukaryotic Cells. (New Haven, CT: Yale University Press).

Martin, W., Rujan, T., Richly, E., Hansen, A., Cornelsen, S., Lins, T., Leister, D., Stoebe, B., Hasegawa, M., and Penny, D. (2002). Evolutionary analysis of *Arabidopsis*, cyanobacterial, and chloroplast genomes reveals plastid phylogeny and thousands of cyanobacterial genes in the nucleus. Proc. Natl. Acad. Sci. USA **99:** 12246–12251.

Matsuzaki, M., et al. (2004). Genome sequence of the ultrasmall unicellular red alga *Cyanidioschyzon merolae* 10D. Nature **428:** 653–657.

Mereschkowsky, C. (1905). Über Natur und Ursprung der Chromatophoren im Pflanzenreiche. Biol. Centralbl. **25:** 593–604.

Mills, C.E., Sedelnikova, S., Søballe, B., Hughes, M.N., and Poole, R.K. (2001). *Escherichia coli* flavohaemoglobin (Hmp) with equistoichiometric FAD and haem contents has a low affinity for dioxygen in the absence or presence of nitric oxide. Biochem. J. **353:** 207–213.

Nakamura, Y., Kanakagiri, S., Van, K., He, W., and Spalding, M.H. (2005). Disruption of the glycolate dehydrogenase gene in the high-CO_2-requiring mutant HCR89 of *Chlamydomonas reinhardtii*. Can. J. Bot. **83:** 820–833.

Nelson, E.B., and Tolbert, N.E. (1970). Glycolate dehydrogenase in green algae. Arch. Biochem. Biophys. **141:** 102–110.

Pellicer, M.T., Badía, J., Aguilar, J., and Baldomà, L. (1996). *glc* locus of *Escherichia coli*: Characterization of genes encoding the subunits of glycolate oxidase and the *glc* regulator protein. J. Bacteriol. **178:** 2051–2059.

Pils, D., and Schmetterer, G. (2001). Characterization of three bioenergetically active respiratory terminal oxidases in the cyanobacterium *Synechocystis* sp. strain PCC 6803. FEMS Microbiol. Lett. **203:** 217–222.

Reumann, S., Ma, C., Lemke, S., and Babujee, L. (2004). AraPerox. A database of putative Arabidopsis proteins from plant peroxisomes. Plant Physiol. **136:** 2587–2608.

Reyes-Prieto, A., Weber, A.P.M., and Bhattacharya, D. (2007). The origin and establishment of the plastid in algae and plants. Annu. Rev. Genet. **41:** 147–168.

Rippka, R., Deruelles, J., Waterbury, J.B., Herdman, M., and Stanier, R.Y. (1979). Generic assignments, strain histories and properties of pure cultures of cyanobacteria. J. Gen. Microbiol. **111:** 1–61.

Shinozaki, A., Sato, N., and Hayashi, Y. (2009). Peroxisomal targeting signals in green algae. Protoplasma **235:** 57–66.

Somerville, C.R. (2001). An early *Arabidopsis* demonstration. Resolving a few issues concerning photorespiration. Plant Physiol. **125:** 20–24.

Staal, M., Lintel-Hekkert, S.T., Harren, F., and Stal, L. (2001). Nitrogenase activity in cyanobacteria measured by the acetylene reduction assay: A comparison between batch incubation and on-line monitoring. Environ. Microbiol. **3:** 343–351.

Stabenau, H., and Winkler, U. (2005). Glycolate metabolism in green algae. Physiol. Plant. **123:** 235–245.

Stenberg, K., Clausen, T., Lindqvist, Y., and Macheroux, P. (1995). Involvement of Tyr24 and Trp108 in substrate binding and substrate specificity of glycolate oxidase. Eur. J. Biochem. **228:** 408–416.

Stenberg, K., and Lindqvist, Y. (1997). Three-dimensional structures of glycolate oxidase with bound active-site inhibitors. Protein Sci. **6:** 1009–1015.

Sueoka, N. (1960). Mitotic replication of deoxyribonucleic acid in *Chlamydomonas reinhardi*. Proc. Natl. Acad. Sci. USA **46:** 83–91.

Tamura, K., Dudley, J., Nei, M., and Kumar, S. (2007). MEGA4: Molecular evolutionary genetics analysis (MEGA) software version 4.0. Mol. Biol. Evol. **24:** 1596–1599.

Thompson, J.D., Higgins, D.G., and Gibson, T.J. (1994). CLUSTAL W: Improving the sensitivity of progressive multiple sequence alignment through sequence weighting, position-specific gap penalties and weight matrix choice. Nucleic Acids Res. **22:** 4673–4680.

Valladares, A., Herrero, A., Pils, D., Schmetterer, G., and Flores, E. (2003). Cytochrome c oxidase genes required for nitrogenase activity and diazotrophic growth in *Anabaena* sp. PCC 7120. Mol. Microbiol. **47:** 1239–1249.

Valladares, A., Maldener, I., Muro-Pastor, A.M., Flores, E., and Herrero, A. (2007). Heterocyst development and diazotrophic metabolism in terminal respiratory oxidase mutants of the cyanobacterium *Anabaena* sp. strain PCC 7120. J. Bacteriol. **189:** 4425–4430.

Walsby, A.E. (2007). Cyanobacterial heterocysts: Terminal pores proposed as sites of gas exchange. Trends Microbiol. **15:** 340–349.

Zelitch, I., Schultes, N.P., Peterson, R.B., Brown, P., and Brutnell, T.P. (2009). High glycolate oxidase activity is required for survival of maize in normal air. Plant Physiol. **149:** 195–204.

Zhao, W.X., Ye, Z., and Zhao, J.D. (2007). RbrA, a cyanobacterial rubrerythrin, functions as a FNR-dependent peroxidase in heterocysts in protection of nitrogenase from damage by hydrogen peroxide in *Anabaena* sp. PCC 7120. Mol. Microbiol. **66:** 1219–1230.

Cyanobacterial Lactate Oxidases Serve as Essential Partners in N_2 Fixation and Evolved into Photorespiratory Glycolate Oxidases in Plants

Claudia Hackenberg, Ramona Kern, Jan Hüge, Lucas J. Stal, Yoshinori Tsuji, Joachim Kopka, Yoshihiro Shiraiwa, Hermann Bauwe and Martin Hagemann

Plant Cell; originally published online August 9, 2011;
DOI 10.1105/tpc.111.088070